www.crt-journal.org

Crystal Research and Technology

Journal of Experimental and Industrial Crystallography
Zeitschrift für experimentelle und technische Kristallographie

WILEY-VCH

Cryst. Res. Technol. **46**, No. 5, 439 – 442 (2011) / **DOI** 10.1002/crat.201000611

Stage B work-hardening of magnesium single crystals

B. Sułkowski[1], R. Chulist[2], B. Beausir[2], W. Skrotzki*[2], and B. Mikułowski[1]

[1] Department of Metallic Materials and Nano-Engineering, Faculty of Non-Ferrous Metals, AGH University of Science and Technology, Al. Mickiewicza 30, 30059 Cracow, Poland
[2] Institute of Structural Physics, Dresden University of Technology, 01062 Dresden, Germany

Received 24 November 2010, revised 11 March 2011, accepted 12 March 2011
Published online 1 April 2011

Key words magnesium, single crystal, work-hardening, EBSD, tilt boundaries.

The change in microstructure during tensile deformation of magnesium single crystals by basal slip was studied with electron backscatter diffraction in the scanning electron microscope. Two samples were plastically deformed up to shear strains of 0.37 and 1.28 belonging to work-hardening stages A and B, respectively. The results show that the local misorientations resulting from rotations around the $<10\bar{1}0>$ axis strongly increase the work-hardening coefficient in stage B. The mechanism of work-hardening in stage B is discussed with respect to subgrain formation.

1 Introduction

Hexagonal close-packed (hcp) metals possess many types of slip and twinning systems with different critical resolved shear stresses. The operating deformation systems depend on the c/a ratio, orientation, temperature and strain rate. Generally, hcp metals can be divided into two groups depending on the c/a ratio [1]. The first group consisting of metals like Mg, Cd, Zn with c/a ratio higher than or close to ideal, 1.633, primarily glides on the basal slip system $(0001)<11\bar{2}0>$. Ti, Zr, Hf with c/a ratio lower than ideal belong to the second group with primary slip taking place on the prismatic slip system $(10\bar{1}0)<1\bar{2}10>$. In single crystals of the first group deformed in so-called "soft orientation" (middle of the standard stereographic triangle), mainly one slip system of type $(0001)<11\bar{2}0>$ is activated [2-7]. Similar to face-centred cubic (fcc) metals the stress-strain curve can be divided into different work-hardening stages suggesting comparable deformation and hardening processes in both crystal structures [8,9]. In particular, in hcp metals the activation of secondary slip is considered in stage B. Theoretical considerations of the activation of secondary slip in hcp metals are given in [10-13]. However, in comparison to fcc metals deformed in multiple slip [15] hcp metals of the first group have not been observed to deform on secondary slip systems [14].

On the other hand, Hirsch and Lally [16] suggested that twins nucleated in regions of high stress concentration can act as barriers to dislocation motion. This aspect is also discussed in [17-19]. The most favourable twin plane for Mg single crystals is $(10\bar{1}2)$, others are $(10\bar{1}1)$, $(30\bar{3}4)$, $(10\bar{1}3)$ [20]. These twinning systems are activated when the single crystal is deformed in compression and tension along or perpendicular to the c-axis, respectively. The nature of deformation twinning in hcp metals is different from that in fcc metals [21].

The aim of the present study is to shed more light on the work-hardening behaviour of Mg single crystals (c/a=1.624) with "soft orientation". This in particular holds for work-hardening in stage B, which is not well-understood so far. Here, electron backscatter diffraction (EBSD) is used as a new technique to investigate the change in local misorientation of Mg single crystals during tensile deformation.

2 Experimental

Magnesium single crystals were grown from extruded rods of 99.8 wt.% purity using the Bridgman method. The growth took place in a split graphite mould under high purity argon at a pressure slightly greater then

* Corresponding author: e-mail: werner.skrotzki@physik.tu-dresden.de

atmospheric. The initial orientation <$\bar{1}212$> parallel to the tensile axis within 2° guaranteed (0001)<$11\bar{2}0$> as primary slip system. Two samples (I and II) with dimensions 3×3×60 mm^3 were deformed in tension at room temperature (T_{def} = 0.32 T_{melt}) with an initial shear strain rate of $10^{-3}s^{-1}$ up to shear strains of 0.37 and 1.28 belonging to stages A and B, respectively (Fig. 1). For EBSD measurements as-grown and deformed samples were first mechanically polished on abrasive paper with graduation 2000 to obtain regular shapes and then electro-polished for 2 h at room temperature in a solution of H_3PO_4 acid and ethanol (volume ratio 3:5) with a tantalum cathode operating at 3 V. The EBSD measurements were carried out in a scanning electron microscope (Zeiss Ultra 55) with field emission gun using a step size of 0.5 μm. Additionally, etch pits on the [$2\bar{1}\bar{1}0$] surface of the initial and deformed material were investigated. The electropolished surface was etched in a solution consisting of 10 g ammonium chloride dissolved in 50 cm^3 water [22].

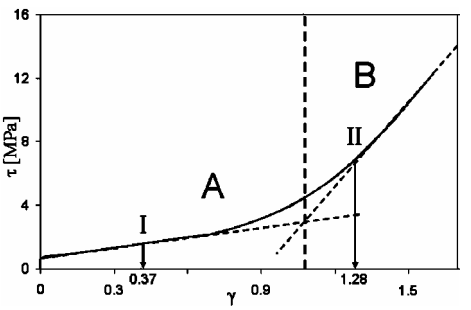

Fig. 1 Typical shear stress τ – shear strain γ curve of magnesium single crystals deformed in tension at room temperature. Single crystals I and II with the same orientation were deformed up to shear strains of 0.37 and 1.28 (marked by arrows) belonging to work-hardening stages A and B, respectively.

3 Results and discussion

Figure 1 shows a typical shear stress – shear strain curve of Mg single crystals investigated in addition to the two samples described in detail in this work. The curve can be roughly divided in two work-hardening stages A and B with reduced work hardening coefficients $\theta_A/G \approx 1.83\times10^{-4}$ and $\theta_B/G \approx 6.71\times10^{-4}$, respectively, ($G = c_{44}$ shear modulus for basal slip). However, the transition from stage A to B is rather gradual. Figure 2 shows the slip lines on two perpendicular surfaces of sample II deformed to γ = 1.28 in stage B. As can be clearly seen within the limit of resolution there are no slip lines belonging to secondary slip systems, in contrast to expectations reported in [10-13].

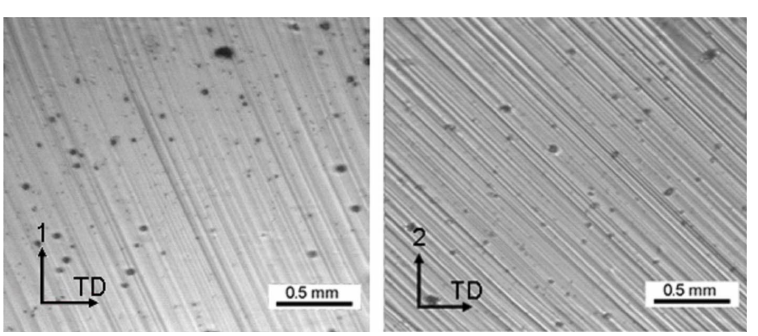

Fig. 2 Optical micrograph showing the slip lines on the two perpendicular surfaces of deformed sample II (TD = [$\bar{1}012$] = tensile direction, 1 = [$41\bar{5}2$] and 2 = [$\bar{2}\,10\,\bar{8}\bar{1}$] = perpendicular directions in planes ($\bar{2}\,10\,\bar{8}\bar{1}$) and ($\bar{1}012$), respectively)

Figure 3a presents (0001), {$1\bar{2}10$}, {$10\bar{1}0$} pole figures of sample II deformed up to γ = 1.28 in the crystal reference system. The orientations (within 12°) cluster on small circles belonging to rotation axes very close to <$10\bar{1}0$> (Fig. 3a). This is also confirmed by the maximum in the inverse pole figure of figure 3b where the misorientation axes calculated between neighbouring measurement points along the tensile direction are given.

To investigate the change in local misorientation along the tensile axis, the misorientation between the measurement point of coordinate (0, 0) and each other points is calculated and depicted in figure 4. The as-grown crystal within the limit of accuracy does not show any misorientation. After γ = 0.37 in stage A the misorientation reaches a maximum value of 3° within bands of 350 μm, while after γ = 1.28 in stage B the misorientation almost continuously increases up to 7° within 550 μm. It is tempting to assume that the misorientation change is related to polygonization of 1/3<$11\bar{2}0$> dislocations gliding on (0001) leading to low

energy dislocation structures in the form of tilt boundaries. The direct observation of etch pits at dislocations in figure 5a-c shows patterns revealing the tilt boundaries formed during deformation.

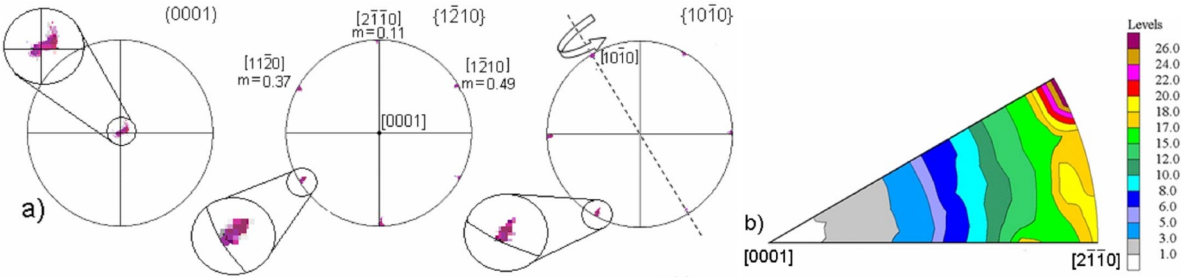

Fig. 3 Pole figures (0001), {1$\bar{2}$10} and {10$\bar{1}$0} of sample II with indicated Schmid factor m for three basal slip systems given in the crystal reference system (a), inverse pole figure of the misorientation axes (b) (Online color at www.crt-journal.org)

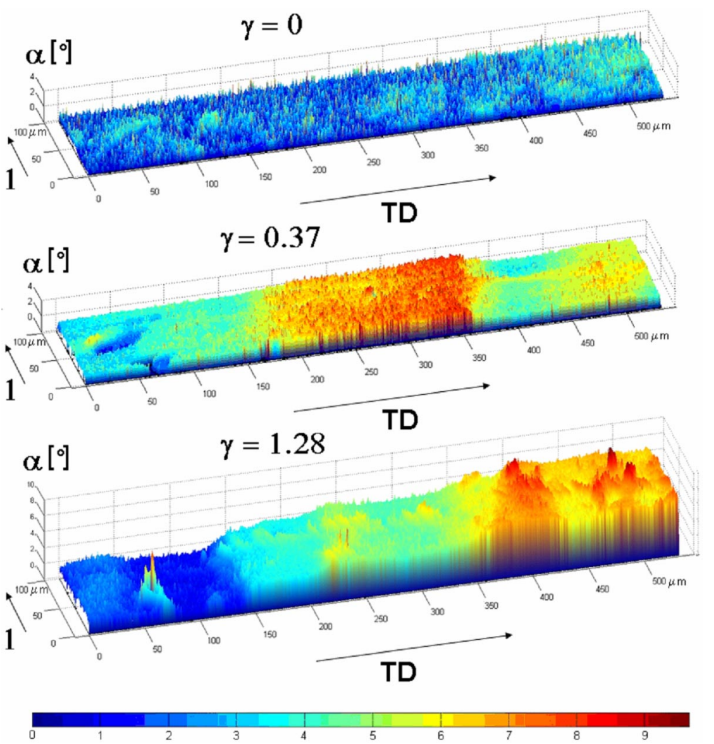

Fig. 4 Misorientation profile of the single crystals investigated (I: γ = 0.37, II: γ = 1.28) with respect to point (0, 0) (α = misorientation angle, TD = tensile direction, 1 = [41$\bar{5}$2] = normal direction in plane ($\bar{2}$ 10 $\bar{8}\bar{1}$).

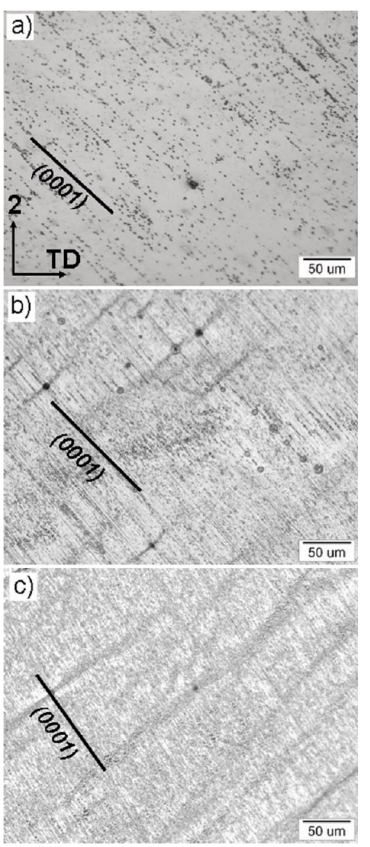

Fig. 5 Optical micrograph showing etch pits of the undeformed (a) and the deformed samples: (b) I: γ = 0.37 and (c) II: γ = 1.28 (TD = [$\bar{1}$012] = tensile direction, 2 = [$\bar{2}$ 10 $\bar{8}\bar{1}$] = perpendicular direction in plane ($\bar{1}$012).

The initial density of etch pits is about 3×10^5cm^{-2} while after γ = 0.37 (stage A) and γ = 1.28 (stage B) it increases to 3×10^6 cm^{-2} and 4.5×10^6 cm^{-2}, respectively. The mean distance between the tilt boundaries decreases during deformation from 138 μm at γ = 0.37 (Fig. 5b) to 62 μm at γ = 1.28 (Fig. 5c). Moreover, the mean length of the tilt boundaries increases from about 70 μm in stage A up to about 400 μm in stage B. This clearly shows that with increasing deformation more tilt boundaries are formed leading to bending of the slip plane by polygonization. The geometrically necessary dislocations result from the constraints on the sample

deformed by single slip in tension. Subgrain formation also was observed by Mikulowski et al. [23] and discussed with respect to vacancy formation during deformation [24]. It is suggested that the increase in work-hardening, which actually is more a gradual increase with strain than a sharp transition between two stages, is due to the decrease of the Schmid factor and the formation of barriers in the form of low angle grain boundaries which reduce the mean dislocation free path.

4 Conclusions

1 No slip systems other than (0001)<11$\bar{2}$0> are activated in stage B work-hardening of Mg single crystals oriented for single slip.
2 The pronounced increase in density and misorientation of low angle boundaries in stage B can be correlated with the increased work-hardening coefficient.
3 As the misorientation axes are almost parallel to <10$\bar{1}$0>, consequently, the low angle tilt boundaries formed during deformation should be composed of edge dislocations with 1/3 <11$\bar{2}$0> Burgers vector.

Acknowledgements The authors acknowledge the support of the Polish Committee for Scientific Research, Agreement No. 18.18.180.481. B. Beausir is grateful to the Alexander von Humboldt Foundation for his research fellowship.

References

[1] R. W. Cahn, P. Haasen, and E. J. Kramer, Materials Science and Technology, Vol. 8 (VCH - Verlagsgesellschaft, Weinheim, 2005).
[2] E. Schmid and W. Boas, Plasticity of Crystals (Hughes & Co, London, 1950).
[3] B. Wielke, W. Tikvic, A. Svobodová, and P. Lukáč, Acta Metall. **25**, 1071 (1977).
[4] B. Mikułowski and B. Wielke, Czech. J. Phys. B **38**, 453 (1988).
[5] B. Wielke, Phys. Status Solidi A **33**, 241 (1976).
[6] E. C. Burke and W. R. Hibbard, Trans. AIME **194**, 295 (1952).
[7] F. F. Lavrentev and Yu. A. Pokhil, Mater. Sci. Eng. **18**, 261 (1975).
[8] S. J. Basinski and Z. S. Basinski, Plastic Deformation and Work Hardening (North Holland Publishing Company, New York, 1979).
[9] M. Boček, Phys. Status Solidi A **3**, 2169 (1963).
[10] P. Lukáč, Czech. J. Phys. B **35**, 275 (1985).
[11] F. F. Lavrentev, Yu. A. Pokhil, and I. N. Zolotukhina, Mater. Sci. Eng. **23**, 69 (1976).
[12] F. F. Lavrentev, Yu. A. Pokhil, and I. N. Zolotukhina, Mater. Sci. Eng. **32**, 113 (1978).
[13] M. H. Yoo, S. R. Angew, J. R. Morris, and K. M. Ho, Mater. Sci. Eng. A **319-321**, 87 (2001).
[14] J. Krásová and P. Kartochvil, Phys. Status Solidi A **7**, 255 (1971).
[15] F. D. Rosi, J. Mater. Sci. **8**, 807 (1973).
[16] P. B. Hirsch and J. S. Lally, Phil. Mag. **12**, 595 (1965).
[17] M. H. Yoo, J. R. Morris, K. M. Ho, and S. R. Agnew, Met. Mater. Trans. A **33**, 813 (2002).
[18] L. Capolungo, I. J. Beyerlein, and C. N. Tomé, Scripta Mater. **60**, 32 (2009).
[19] D. Phelan, N. Stanford, B. Thijsse, and J. Sietsma, Mater. Sci. Forum **638-642**, 1585 (2010).
[20] H. Yoshinaga, T. Obara, and S. Morozumi, Mater. Sci. Eng. **12**, 255 (1973).
[21] M. S. Szczerba, T. Bajor, and T. Tokarski, Phil. Mag. **84**, 481 (2004).
[22] M. Sasaki and K. Marukawa, Trans. JIM **18**, 540 (1977).
[23] B. Mikułowski and M. Książek, Key Eng. Mater. **97-98**, 395 (1995).
[24] M. Zehetbauer and B. Mikułowski, Arch. Metallurgy **46**, 65 (2001).

